Frequency Domain Analysis of Acoustic Emission Signals in Medical Drill Wear Monitoring

Zrinka Murat[1], Danko Brezak[1], Goran Augustin[2] and Dubravko Majetic[1]
[1]*Faculty of Mechanical Engineering and Naval Architecture, University of Zagreb, Ivana Lucica 5, Zagreb, Croatia*
[2]*University Hospital Center Zagreb and School of Medicine, University of Zagreb, Kispaticeva 12, Zagreb, Croatia*

Keywords: Bone Drilling, Drill Wear, Acoustic Emission, Neural Networks, Data Mining.

Abstract: Medical drills are subject to wear process due to mechanical, thermal and, potentially, sterilisation influences. The influence of drill wear on friction contributes to the drilling temperature rise and occurrence of thermal osteonecrosis. During the cutting process drilling temperature cannot be adequately reduced by applying cooling fluid externally on the bone surface and a part of a tool which is not in the contact with the bone if higher wear rates occurs. Since it is not possible to directly establish or measure drill wear rate without interrupting the machining process, this important parameter should be estimated using available process signals. Therefore, the application of tool wear features extracted from acoustic emission signals in the frequency domain for the purpose of indirect medical drill wear monitoring process has been studied in detail and the results are presented in this paper.

1 INTRODUCTION

Beside several important factors related to the drill design, machining parameters, drilling depth, and cooling technique, drill wear rate is one of the most influential factors in temperature increase during bone drilling and potential occurrence of thermal osteonecrosis. Medical drills wear out due to the mechanical, and potentially also chemical and thermal factors which occur during sterilization and continuous application in different cutting conditions. Higher wear rate induces higher friction in the cutting zone, and consequently higher forces and heat generation. This logical and a well-known relationship has been confirmed several decades ago by Mathews and Hirsch, 1972, when they compared new drills with the used one which drilled more than 200 holes. As expected, worn drills caused higher temperatures during drilling.

Importance of a drill wear rate on bone thermal damages has been also emphasised in the more recent study performed by Allan, Williams, and Kerawala, 2005, where three types of drills were compared: new one, drill which drilled 600 holes, and drill which were used for several months. The results have shown important differences in mean temperature rise values – from 7.5°C (unworn drill) to 25.4°C (completely worn drill), measured in relation to the initial bone temperature of 37°C. Authors suggested drill replacement after every surgical intervention.

The same negative influence of drill wear has been reported in Chacon et al., 2006, Querioz et al., 2008, and Jochum and Reichart, 2000, where the temperature rise and thermal osteonecrosis is noticed after only 25, 30 and 40 drilled holes, respectively.

According to the Singh, Davenport and Pegg, 2010, whose research included 40 hospitals in the Great Britain, 75% of them had no guidelines for controlling and maintenance of medical drills. The remaining 10 hospitals confirmed they have instructions related to the identification and labelling of worn drills, and 8 of them confirmed that they actually implemented those regulations. From the total number of hospitals, 45% of them said that they use single-used medical drills. At the end of their report authors point to the frequent application of worn drills, as well as the absence of any consensus regarding the tool wear inspection.

Although there has been many papers published in the past 25 years considering tool wear monitoring and identification in industrial applications (Jantunen, 2002), comprehensive analyses in the field of medical drilling are still missing. Industrial drilling dynamics usually differ from the one in medical applications in view of

Murat Z., Brezak D., Augustin G. and Majetic D.
Frequency Domain Analysis of Acoustic Emission Signals in Medical Drill Wear Monitoring.
DOI: 10.5220/0006150401730177
In *Proceedings of the 10th International Joint Conference on Biomedical Engineering Systems and Technologies (BIOSTEC 2017)*, pages 173-177
ISBN: 978-989-758-212-7

different drill characteristics, machining parameters, and workpiece material characteristics. Therefore, it is necessary to establish the possibility of applying some of the proposed industrial solutions to medical drill wear monitoring. First analyses have confirmed the applicability of multi-sensor concept and advanced decision algorithms in the on-line medical drill wear monitoring (Staroveski et al., 2014, Staroveski, Brezak and Udiljak, 2015).

In one of those two studies (Staroveski, Brezak and Udiljak, 2015) two types of signals were analysed: servomotor currents and acoustic emission. The acoustic emission signals were roughly processed in a way that each signal was fragmented in the frequency domain into 7 samples (between 50-400 kHz). Each sample was related to the belonging 50 kHz frequency bandwidth (50-100, 100-150;...; 350-400 kHz). Drill wear features were then extracted from every sample individually. Since there was only one, arbitrarily chosen bandwidth (50 kHz), additional analysis with different frequency bandwidths has been performed in this study in order to determine the full potential of AE signals in surgical drill wear monitoring.

The paper is organised as follows. Section 2 describes experimental setup and parameters used in data acquisition process, while Section 3 explains a method for drill wear feature extraction from measured AE signals. In Section 4 neural network classifier algorithm is briefly presented, and Section 5 includes drill wear rate classification results. Concluding remarks are finally summarised in Section 6.

2 EXPERIMENTAL DETAILS

Acoustic emission (AE) signals have been measured during bone drilling on the 3-axis bench-top mini milling machine adjusted for the purpose of this research (Figure 1). The machine has been retrofitted with the 0.4 kW (1.27 Nm) permanent magnet synchronous motors with integrated incremental encoders (type Mecapion SB04A), corresponding motor controllers (DPCANIE-030A400 and DPCANIE-060A400), ball screw assemblies, and LinuxCNC open architecture control (OAC) system. AE signals were measured using Kistler piezoelectric industrial accelerometer type 8152B1 coupled with 5125B interface module. The sensor was mounted on the flange used to attach main spindle motor to Z-axis, near the motor front bearing and the drill. Its measuring range was from 50 to 400 kHz.

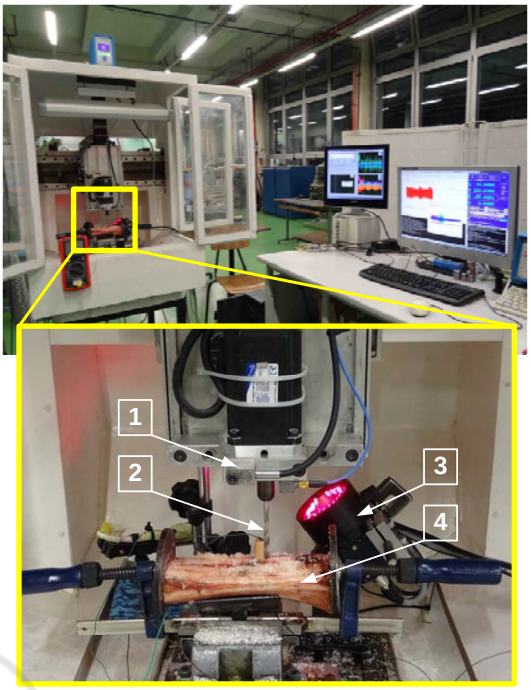

1) Acoustic emission sensor
2) Medical drill
3) Industrial CCD camera with telecentric lens system
4) Bovine bone specimen

Figure 1: Experimental setup.

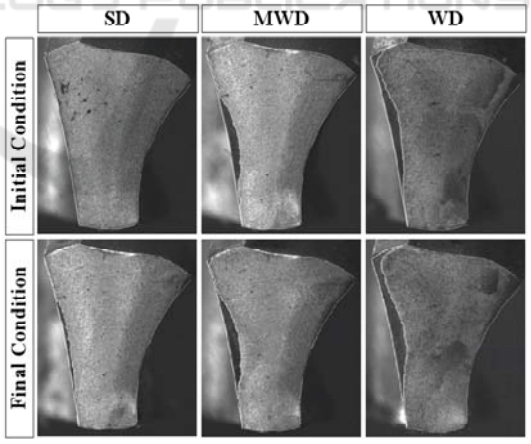

Figure 2: Images of cutting edges at the beginning and at the end of the drilling experiment with the sharp drill (SD), medium worn drill (MWD) and worn drill (WD). Drill wear is observable as a dark area along the cutting edge on the drill flank.

Three types of standard, 4.5 mm in diameter, medical drills (Komet Medical Gmbh, S2727.098) with two flutes and a point angle of 90° were used in

the experiment. They only differed in the amount of drill flank wear level (Figure 2). First type belonged to a group of sharp drill (SD), second type was categorised as a medium worn drill (MD), and third type was defined as a worn drill (WD). Drilling temperature for WD type of a drill exceeded 55°C in almost all measured samples.

Three cutting speed values were combined with four different feed rates (Table 1), and for each of those twelve combinations of machining parameters ten measurements were performed using randomly selected approach (two consecutive measurements had different machining parameters). Altogether, 360 sets of data (120 sets for each drill wear level - SD, MWD, WD) have been recorded.

Table 1: Combinations of machining parameters.

Cutting speed (v_c), Rotational speed*		Feed rate (f)			
		mm/rev			
		0.01	0.03	0.05	0.1
m/min	rev/min*	mm/s			
10	707.4	0.12	0.35	0.59	1.18
30	2122.1	0.35	1.06	1.77	3.54
50	3536.8	0.59	1.77	2.95	5.90

Bone specimens were prepared using fresh bovine tibia with average diaphysis cortical thickness (drilling depth) of 8.5 mm and variable mechanical properties (hardness). AE signal sample was taken during one cortical bone drilling layer, and when drill entered into cancellous bone it was removed from the hole, moved along Y-axis for 5 mm and positioned for the next drilling operation.

3 DRILL WEAR FEATURES EXTRACTION

Samples of AE signals were taken using multi-function high-speed data acquisition I/O board PCI-DAS4020/12. For every hole, signals were measured for 0.1 second with the sampling rate of 2 MHz after both cutting edges completely entered into the cortical bone. Measured AE signals were then analysed in the frequency domain using Fast Fourier transform (FFT) method. Analyses were performed within the AE sensor measuring range (50-400 kHz).

Each signal has been divided into a series of samples depending on a chosen frequency bandwidth, and for each sample power spectrum density (PSD) was established. Since in Staroveski, Brezak and Udiljak, 2015, a 50 kHz frequency bandwidth was used, six additional and different bandwidths (5, 10, 15, 20, 30, and 40 kHz) were analysed in this study. In another words, in the case of 5 kHz bandwidth we got 70 samples per signal (each sample related to 70 different bandwidths within the 50-400kHz interval), while for 40 kHz bandwidth signal was divided into 9 samples, i.e., 50-90 kHz, 90-130 kHz, ..., 330-370kHz, and 370-400 kHz (the last sample had 30 kHz bandwidth because the upper frequency value cannot exceed sensor measurement range of 400 kHz).

Energy of each sample of the analysed AE signal has been calculated from the expression

$$\psi^2 = \int_{f_L}^{f_U} S_y \, df \,, \tag{1}$$

where S_y is one-sided PSD function of the AE signal, while f_L and f_U are lower and upper frequency values chosen to reflect the energy in the range of interest (Scheffer, Heyns and Klocke, 2003).

Energy values of all samples of AE signals were used together with the belonging combination of feed rate and cutting speed as drill wear features in the classification of one of three analysed drill wear conditions (SD, MWD, WD).

4 NEURAL NETWORK CLASSIFIER

Drill wear level classification was performed by using a well-known three-layered feed-forward Radial Basis Function Neural Network (RBFNN). This type of a neural network has good classification capabilities and can be trained in one step with simple hidden layer structure adaptation in view of the learning problem.

In the training phase matrix of synaptic weights $\boldsymbol{c}$ is calculated from the expression:

$$\boldsymbol{c} = \boldsymbol{H}^{-1}\boldsymbol{y} \,, \tag{2}$$

where $\boldsymbol{y}$ stands for the matrix of desired output values and $\boldsymbol{H}$ is the matrix of hidden layer neurons (RBF activation functions) outputs. Since Gauss function was used as an activation function in this study, elements of matrix $\boldsymbol{H}$ are determined using the expression:

$$H_{ij} = exp\left(\frac{-\left\| \mathbf{x}_i - \boldsymbol{t}_j \right\|^2}{\sigma_j^{\,2}} \right), \; i=1, ..., N, \; j=1, ..., K, \tag{3}$$

where $\mathbf{x}_i$ is a vector composed from ith element of all (L) input vectors, $\boldsymbol{t}_j$ is a jth hidden layer neuron

position center vector, and σ_j is an activation or RBF function width of the *j*th hidden layer neuron.

Gaussian widths are calculated as a geometrical mean value of the Euclidean distances of the centre of the *j*th neuron and the centers of two of his neighbor neurons:

$$\sigma_j = \sqrt{p_{1j}\, p_{2j}}\,, \tag{4}$$

where p_{1j} is the Euclidean distance between the *j*th neuron centre and the (*j-1*)th neuron centre, and p_{2j} is the Euclidean distance between the *j*th neuron centre and the (*j+1*)th neuron centre.

Matrix $\boldsymbol{H}$ was quadratic matrix in this study, since the number of hidden layer neurons was equal to the number of data set samples used in the training phase ($K = N$).

In the testing phase, matrix or, in this case, three-element vector of desired output values $\boldsymbol{y}$ is obtained from the expression:

$$\boldsymbol{y} = \boldsymbol{H}\boldsymbol{c}\,. \tag{5}$$

Before entering in the training phase, all classifier input data values were normalised in the interval (0, 1). Elements of vector $\boldsymbol{y}$ or classifier outputs were defined as either "0" or "1", depending on the drill wear level class to which analysed combination of input features belonged to (network output belonging to the actual class was defined as "1" and the remaining two outputs as "0").

5 RESULTS AND ANALYSIS

For every combination of RBFNN inputs, 360 data sets have been prepared. They were then divided into two groups, where 180 sets were used in the RBFNN classifier training phase, and the remaining 180 in its testing phase. Data used in the testing phase were additionally divided into 5 groups or tests (T1 – T5). Each group was composed from 36 samples belonging to each of 36 different combinations of machining parameters and drill wear levels (three cutting speed values combined with four different feed rates and three drill wear levels).

Performance analysis of drill wear features has been carried out in two steps. At first, energy values belonging to every analysed frequency bandwidth of the AE signals were individually analysed in combination with machining parameters using RBFNN classifier. Results were compared using performance index defined as Classification Success Rate (CSR), i.e., the ratio of successfully classified samples to all tested samples.

All those features which satisfied minimal predefined CSR value (CSR_min) were taken in the second phase of the analysis. Based on the CSR values obtained for all drill wear features individually, two CSR limits have been established: CSR_min = 50% and CRS_min = 60%.

In the second phase of this analysis, features that satisfied abovementioned conditions were mutually combined and tested again. Classification success rates of those combinations are presented in Tables 2, 3, and 4. Features were first combined for each analysed frequency bandwidth separately (Table 2 and 3) and then additionally regardless to the bandwidth association (Table 4).

Table 2: Classification success rates of tests composed of all drill wear features (AE signal energies) of the analysed frequency bandwidth that individually fulfilled condition CSR_min ≥ 50%.

Frequency bandwidth, kHz	CSR of the tests, %					
	T1	T2	T3	T4	T5	Avg.
5	97.2	97.2	94.4	100	94.4	96.6
10	94.4	94.4	86.1	97.2	97.2	93.9
15	94.4	88.9	97.2	97.2	94.4	94.4
20	94.4	97.2	88.9	94.4	97.2	94.4
	100	97.2	94.4	91.7	94.4	95.6
40	91.7	91.7	86.1	91.7	94.4	91.1

Table 3: Classification success rates of tests composed of all drill wear features (AE signal energies) of the analysed frequency bandwidth that individually fulfilled condition CSR_min ≥ 60%.

Frequency bandwidth, kHz	CSR of the tests, %					
	T1	T2	T3	T4	T5	Avg.
5	91.7	88.9	100	97.2	94.4	94.4
10	94.4	97.2	88.9	97.2	100	95.6
15	97.2	97.2	94.4	94.4	100	96.7
20	94.4	88.9	100	88.9	91.7	92.8
30	97.2	94.4	97.2	94.4	91.7	95.0
40	91.7	83.3	91.7	77.8	83.3	85.6

Table 4: Classification success rates of tests composed of all drill wear features (AE signal energies) of all analysed frequency bandwidths that individually fulfilled condition CSR_min ≥ 50% and CSR_min ≥ 60%.

CSR_min, %	CSR of the tests, %					
	T1	T2	T3	T4	T5	Avg.
50	97.2	97.2	91.7	91.7	97.2	95.0
60	86.1	88.9	94.4	91.7	97.2	91.7

Practically all combinations of energy features

related to each frequency bandwidth separately accomplished high classification success rate of more than 90% (Table 2 and 3). However, if the results from Table 2 (CSR_min = 50%) are compared with the one presented in Staroveski, Brezak and Udiljak, 2015, (Table 5) where frequency bandwidth was 50 kHz, a slight improvement in classifier accuracy can be observed, particularly in the case of the features extracted from the samples with narrowest bandwidth of 5 kHz.

Table 5: Classification success rates of tests composed of all drill wear features (AE signal energies) of the 50 kHz frequency bandwidth that individually fulfilled condition CSR_min ≥ 50% (Staroveski, Brezak and Udiljak, 2015).

Frequency bandwidth, kHz	CSR of the tests, %					
	T1	T2	T3	T4	T5	Avg.
50	86.1	91.7	94.4	86.1	91.7	90

Combination of energy features from different frequency bandwidths (Table 4) obtained very similar results to those presented in Table 2 and 3.

6 CONCLUSIONS

Analysis of medical drill wear features extracted from the AE signals in the frequency domain using different frequency bandwidths has been presented in this study. Features were used to identify one of the three drill wear levels. Application of the AE signals in medical drill wear monitoring can be very useful due to the fact that that type of the signal has already shown insensitivity to variations of bone mechanical properties. This study has additionally confirmed high precision of the AE signals in drill wear level classification from sharp to completely worn drill. Although only slight improvement has been observed in comparison with the results from one of the previous study (around 6% higher classification precision), it can nevertheless positively contribute to the design of a reliable and precise multi-sensor medical drill wear estimators. Their purpose would be to reduce mechanical and thermal bone damages in the case of fully automated next-generation bone drilling machines applications.

ACKNOWLEDGEMENTS

This work has been fully supported by the Croatian Science Foundation under the project number IP-09-2014-9870.

REFERENCES

L. S. Mathews, C. Hirsch, 1972, *Temperature measured in human cortical bone when drilling*, The Journal of Bone Joint Surgery, 54-A, pp. 297-308.

W. Allan, E. D. Williams, C. J. Kerawala, 2005, *Effects of repeated drill use on temperature of bone during preparation for osteosynthesis self-tapping screws*, British Journal of Oral and Maxillofacial Surgery, 43, pp. 314-319.

G. E. Chacon, D. L. Bower, P. E. Larsen, E. A. McGlumphy, F.M. Beck, 2006, *Heat Production by 3 Implant Drill Systems After Repeated Drilling and Sterilization*, Journal of Oral and Maxillofacial Surgery, 64, pp. 265-269.

T. P. Queiroz, F. Á. Souza, R. Okamoto, R. Margonar, V. A. Pereira-Filho, I. R. Garcia, E. H. Vieira, 2008, *Evaluation of Immediate Bone-Cell Viability and of Drill Wear After Implant Osteotomies: Immunohistochemistry and Scanning Electron Microscopy Analysis*, Journal of Oral and Maxillofacial Surgery, 66, pp. 1233-1240.

R. M. Jochum, P. A. Reichart, 2000, *Influence of multiple use of Timedur® – titanium cannon drills: thermal response and scanning electron microscopic findings*, Clinical Oral Implants Research, 11, pp. 139-143.

J. Singh, J. H. Davenport, D. J. Pegg, 2010, *A national survey of instrument sharpening guidelines*, The Surgeon, 8, pp. 136-139.

E. Jantunen, *A summary of methods applied to tool condition monitoring in drilling*, 2002, International Journal of Machine Tools & Manufacture, 42, pp. 997-1010.

T. Staroveski, D. Brezak, V. Grdan, T. Bacek, 2014, *Medical Drill Wear Classification Using Servomotor Drive Signals and Neural Networks*, Lecture Notes in Engineering and Computer Science, 2211 (1), pp. 599-603.

T. Staroveski, D. Brezak, T. Udiljak, 2015, *Drill wear monitoring in cortical bone drilling*, Medical engineering & physics, 37 (6), pp. 560-566.

C. Scheffer, P. S. Heyns, F. Klocke, 2003, *Development of a tool wear-monitoring system for hard turning*, International Journal of Machine Tools and Manufacturing,43, pp.973–85.